Evaluation of malachite green and methyl violet dyes removal by 3A molecular sieve adsorbents

Sharmeendran Muniandy, Liza Salleh, Muhammad Abbas Ahmad Zaini*

Center of Lipids Engineering and Applied Research (CLEAR), Ibnu-Sina Institute for Scientific and Industrial Research, Universiti Teknologi Malaysia, 81310 UTM Johor Bahru, Johor, Malaysia, email: abbas@cheme.utm.my (M.A.A. Zaini)

ABSTRACT

This work was aimed at evaluating cationic dyes adsorption properties of 3A-molecular sieve adsorbents. Two cationic dyes, namely malachite green and methyl violet were used to probe the adsorbent performance. The adsorbents were characterized for surface functional groups, thermal stability, and specific surface area. The unmodified 3A-molecular sieve showed a surface area of 0.195 m²/g, whereas the value decreased upon sodium hydroxide treatment. The kinetics data fitted well into the pseudo-first-order model, suggesting a physical adsorption process via diffusion-limited transport mechanism, whereby cation-exchange and electrostatic attraction are the possible removal mechanisms. The modified adsorbent revealed better removal capacities for both dyes at 136 and 186 mg/g for methyl violet and malachite green, respectively. The Langmuir model adequately described the equilibrium data, indicating a homogenous nature of monolayer adsorption. The 3A-molecular sieve adsorbents could be effectively used as adsorbent for cationic dyes removal.

Keywords: Adsorption; Malachite green; Methyl violet; 3A-molecular sieve

1. Introduction

Industrial development in recent decades has left various negative effects to the environment. Environmental pollution has become the main concern for dyes manufacturers and production industries. Dyes are important because of their wide-spread demand to instil aesthetic colours in different commodities like leather, textile, rubber, cosmetics, paper, and food. About 15% of the total production is normally lost as effluent during the production and dyeing processes [1]. Dyes in water are toxic, and pose serious environmental threat to aquatic creatures and human health. Consequently, the aquatic ecosystem is compromised because oxygen and sunlight are insufficient for respiration and photosynthesis activities. Therefore, the removal of dye pollutants from water is of vital importance. Hence, suitable treatment methods are required to bring the contaminated water to an acceptable concentration and toxicity level [2].

Dye removal techniques such as photodegradation, membrane filtration, adsorption, and biological treatment are available for dyes decolorization and removal [1,3]. Adsorption process outwits the other removal strategies due to its low cost, and simplicity of operation and design. The most commonly used solid adsorbent is activated carbon due to its porous structure which allows an extensive adsorption capacity for many kinds of pollutants [4]. Nevertheless, the high production cost of activated carbon restricts its wide applicability in wastewater treatment. Thus, there is an increasing need to quest for cheap alternative and effective dye adsorbents [5,6].

Molecular sieves are zeolites with crystalline, three dimensional molecules with surface pores, and channels that can selectively adsorb molecules of certain size and shape. The specific cation in molecular sieve influences its adsorptive properties and pore diameter. For example, 3A-molecular sieve is composed of aluminosilicate compound which

* Corresponding author.

adsorbs molecules with critical diameter of less than 3 Å (0.3 nm), such as hydrogen, helium, and CO. The adsorption properties of molecular sieve adsorbents, such as 3 A [7,8], 4 A, and 5 A [9], Ni-SBA-16 [10] and MCM-41 [11] for organic compounds and dyes removal with promising performance have been documented in literature.

Acid treatment of zeolites is an established method to alter the SiO_2/Al_2O_3 ratio in zeolite framework, and so the adsorption properties [12]. However, the effect of base treatment on the adsorption properties of zeolite for dyes removal is still lack in much of published works. Therefore, this work was aimed to evaluate the performance of 3A molecular sieve and its base-modified derivative by mild sodium hydroxide solution in dyes adsorption. As opposed to acid treatment which selectively dissociates the framework of Al atoms, the base treatment is expected to preferentially remove siliceous species from the zeolitic structure. As a result, uniform mesopore structures are formed, without affecting the microporous structure of adsorbent [13]. In this work, the effects of dye concentration and contact time were studied, and the adsorption data were analyzed to shed some light into possible mechanisms of adsorption by 3A molecular sieve adsorbents.

2. Materials and methods

3A-molecular sieve (potassium–sodium aluminosilicate, $K_nNa_{12-n}[(AlO_2)_{12}(SiO_2)_{12}] \times H_2O$) was obtained from Sigma-Aldrich (Darmstadt, Germany). Malachite green and methyl violet dyes were supplied by R&M Chemicals (Essex, UK). Fig. 1 shows the molecular structure and size of dyes. NaOH was purchased from QRec (Selangor, Malaysia). 3A-molecular sieve (3A-MS) was soaked in 0.2 M NaOH solution, and the mixture was heated at 80°C for 5 h. Then, the solid was filtered using a vacuum filter and dried in an oven at 100°C for 24 h prior to use.

The adsorbents were characterized for thermal decomposition using a Perkin-Elmer (Massachusetts, USA) thermogravimetric analyzer (TGA 7) under nitrogen flow of 10 mL/min and heating rate of 10°C/min. The specific surface area was determined using a Brunauer–Emmett–Teller surface area analyzer (ASAP 2020) at liquid nitrogen temperature of 77 K. The surface chemistry of adsorbents was obtained using a Perkin-Elmer (Massachusetts, USA) Fourier

transform infrared spectrometer. The pH of adsorbents was determined by adding 1 g of adsorbent into a beaker bearing 100 mL of distilled water. The mixture was heated at 100°C for 15 min, and allowed to cool at room temperature prior to pH measurement using a portable pH meter (HI 9813-5, Hanna Instruments, Rhode Island, USA).

For equilibrium adsorption, 50 mg of adsorbent was brought into contact with 50 mL of dye solution of varying initial concentrations (2–400 mg/L) for 48 h. The residual concentrations were measured using a HALO VIS-10 spectrophotometer at wavelengths of 619 nm (a.u. = 0.0543 × concentration, R^2 = 0.9931) and 586 nm (a.u. = 0.0445 × concentration, R^2 = 0.9979) for malachite green and methyl violet, respectively. The adsorption capacity at equilibrium, q_e (mg/g) was calculated as, $q_e = (C_0 - C_e) \times (V/m)$, where C_0 and C_e (mg/L) are the initial and equilibrium concentrations respectively, V (L) is the volume of dye solution, and m (g) is the mass of the adsorbent. For adsorption kinetics, six concentrations ranging from 2 to 25 mg/L were assessed, and the residual concentrations were measured at the pre-set time intervals. The adsorption capacity at time t, q_t (mg/g) was calculated as, $q_t = (C_0 - C_t) \times (V/m)$, where C_t (mg/L) is the measured concentration at time, t.

3. Results and discussion

3.1. Characteristics of adsorbents

The modified 3A-MS shows a slight decrease in yield of 97.3% upon NaOH treatment. The values of specific surface area were measured as 0.195 and <0.100 m²/g for 3A-MS and the base-modified one, respectively. Both adsorbents possess a basic surface with pH values of 10.

Fig. 2 displays the thermogravimetric profiles of adsorbents. The weight loss was recorded at 100°C to 274°C, with two peaks centred at 168°C. This is associated with the dehydration of water from the adsorbents. The two adsorbents carry similar amounts of free moisture (5% at 100°C) and bound water (13% at 274°C). This signifies the hygroscopic attribute of 3A-MS to adsorb moisture from the surrounding, which remains unchanged upon the base treatment. Furthermore, weight loss at 230°C could also be attributed to the dehydration of water hydrating metal cation, Al^{3+}. A small weight loss in the range of 500°C–800°C is likely due to the loss of volatiles from the building matrix

Malachite green ($C_{23}H_{25}ClN_2$),
molecular weight = 365 g/mol,
molecular diameter = 0.82 nm

Methyl violet ($C_{24}H_{28}ClN_3$),
molecular weight = 394 g/mol,
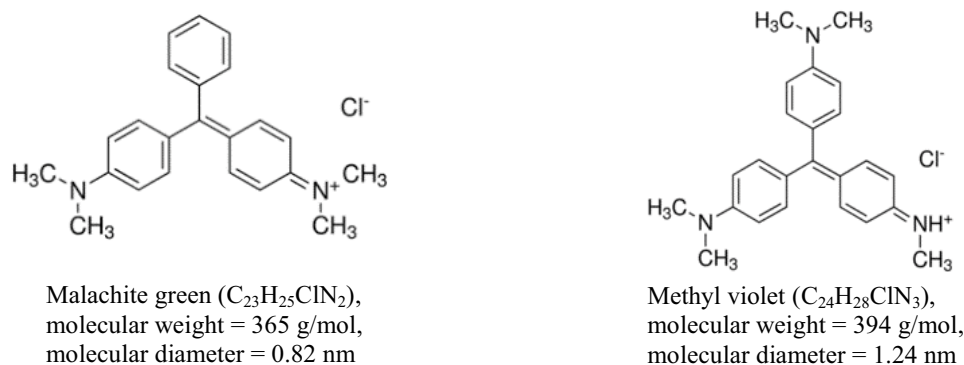molecular diameter = 1.24 nm

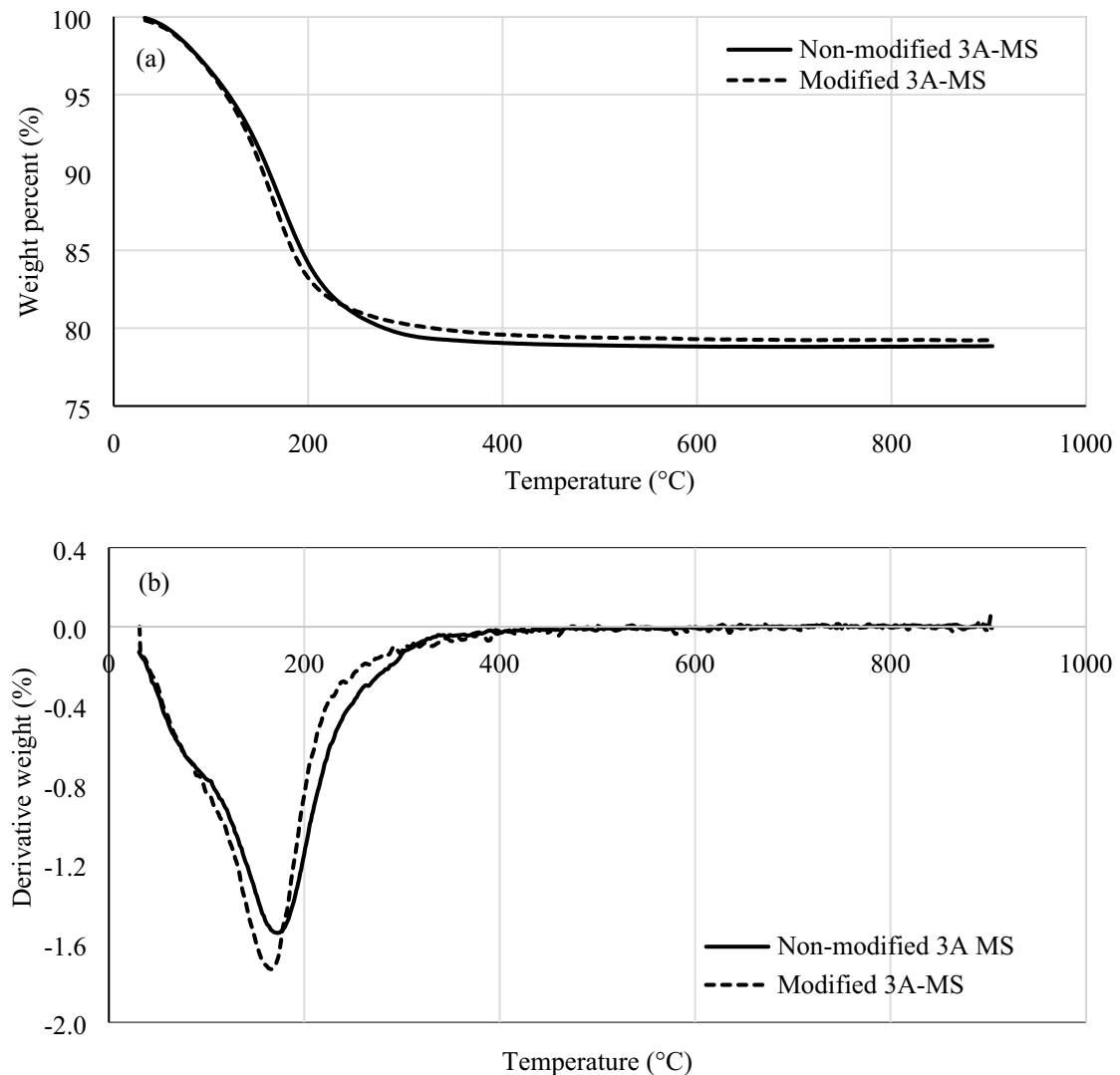Fig. 1. Molecular structures of malachite green and methyl violet dyes.

Fig. 2. Thermogravimetric profiles of adsorbents, (a) weight loss and (b) derivative weight loss.

of adsorbents [14]. The residual weight of 79% at 900°C implies the thermal stability of potassium–sodium aluminosilicate crystalline structure. The modified adsorbent exhibits a slightly higher water content due to the post-adsorbed water, and a slightly lower residual weight as a result of minor structural change during NaOH treatment.

Fig. 3 shows the vibration modes of different functional groups in the FTIR spectra of 3A-MS adsorbents. The stretching and bending as interpreted from the spectrum are mainly associated with the presence of Si–O–Al and Si–O–Si bonds in the aluminosilicate material [15]. The bands in the range of 750–600 cm^{-1} are attributed to the pseudo-crystalline vibrations of exchangeable cations. However, the intensity decreases due to partial desilication as well as loss of crystallinity after modification. Besides, the peak at 968 cm^{-1}, and that shifted to 970 cm^{-1} after NaOH treatment signify the presence of –Al–O bond [16]. The sharp peaks around 550 cm^{-1} represent skeletal vibrations of Al–Si–O bonds present in 3A-MS non-modified

adsorbent. Similarly, the peaks intensity decreases due to desilication by base solution.

3.2. Adsorption studies

Fig. 4 displays the rate of dyes adsorption by 3A-MS adsorbents. Generally, the adsorption increases with increasing contact time until the surface of adsorbents attains equilibrium at which the q_t remains nearly unchanged. Obviously, the values of q_t increased with increasing dyes concentrations. The concentration gradient of solution provides sufficient driving force to overcome the mass transfer resistance at the solid phase. This is generally associated with the number of available active sites to accommodate dye molecules on the adsorbent surface. However, the adsorption rate decreases with contact time while approaching equilibrium due to depleting bulk concentration and repulsion forces created by the already adsorbed molecules on the adsorbent.
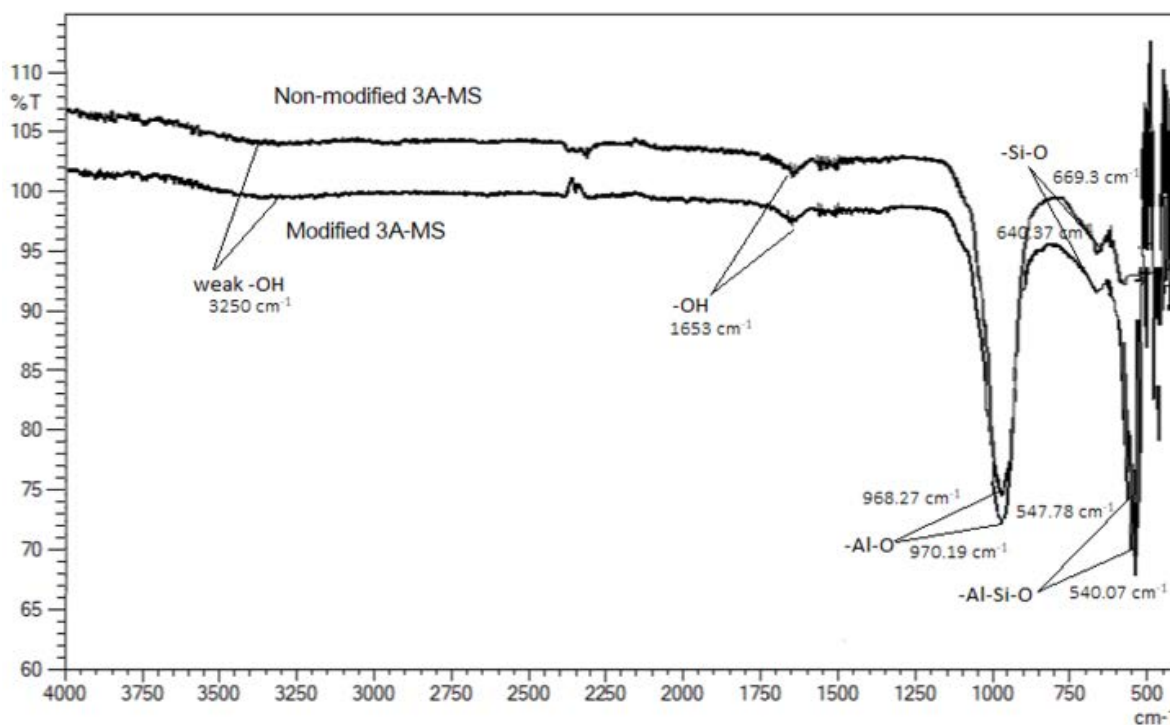
Fig. 3. FTIR spectra of 3A-MS adsorbents.

The increase in malachite green dye concentration has resulted in the increase of contact time to reach equilibrium, which explains the restriction of access due to molecules competition for active sites. For malachite green adsorption at C_0 = 25 mg/L, 3A-MS requires 250 min to reach equilibrium as opposed to 140 min at C_0 = 15 mg/L. For methyl violet adsorption, a longer but similar equilibrium time of 350 min was recorded at three concentrations studied for both adsorbents. From Fig. 4, the modified 3A-MS shows only a slight improvement for malachite green removal at C_0 = 25 mg/L, in which the q_t increased from 10.7 to 13.9 mg/g.

Fig. 5 shows the rate of methyl violet adsorption onto modified 3A-MS. From Fig. 5a, there is no apparent dye removal at concentrations of 2 and 5 mg/L, well before 51 and 33 min, respectively. The same pattern was also observed for methyl violet adsorption by 3A-MS, and malachite green adsorption by both adsorbents at the same concentrations (figures not shown). The S-shaped kinetics behavior could be due to the non-porous nature of 3A-MS adsorbents (surface area ≤ 0.2 m²/g) and very slow diffusion at lower concentrations. As the concentration increases, the dye molecules are no longer constrained in the bulk solution, and therefore could easily diffuse and access the available vacant sites for adsorption to take place as depicted in Fig. 5b.

The adsorption rate data were fitted into pseudo-kinetics models, and the constants are summarized in Table 1. The pseudo-first-order and pseudo-second-order models are given as, $q_t = q_e(1-e^{-k_1t})$ and $q_t = q_e^2 k_2 t/(1 + q_e k_2 t)$, respectively, where k_1 (1/min) and k_2 (g/mg min) are the rate constants. The adsorption of dyes at lower concentrations (2, 5, and 10 mg/L) did not satisfactorily fit into the pseudo-kinetics models as a result of weak driving force to shorten the length of diffusion path and to promote the transport of dye molecules toward the adsorbent surface (Fig. 5a). From Table 1, the pseudo-first-order model shows a good fit with dyes adsorption data, with higher R^2 values and model q_e values close to the experimental ones.

The applicability of this model suggests that the adsorption is a physical process via diffusion-limited transport mechanism [17], by which external (film) diffusion could be the rate-controlling step. The rate constant, k_1 values for malachite green adsorption are between 0.006 and 0.016 1/min, while for methyl violet are in the range of 0.006 to 0.008 1/min. A higher rate constant signifies a greater affinity of malachite green adsorption toward 3A-MS adsorbents.

Fig. 6 shows the removal performance of 3A-MS adsorbents. In general, the adsorption capacity increases with initial dye concentration to a point where the surface reaches its saturation limit to yield the maximum adsorption capacity.

At malachite green concentration of 410 mg/L, the modified 3A-MS demonstrates a 181 mg/g removal capacity, that is slightly greater than the unmodified one (175 mg/g). Similarly, at C_0 = 534 mg/L, the modified 3A-MS shows a methyl violet capacity of 128 mg/g, as compared to 114 mg/g by its counterpart. The increase in adsorption capacity upon NaOH treatment could be caused by partial desilication of crystallinity structure, thus exposing the active centres for adsorption.

The 3A-MS adsorbents exhibit a comparable efficiency of 96% for malachite green removal at concentrations up to 25 mg/L. The performance gradually declines to
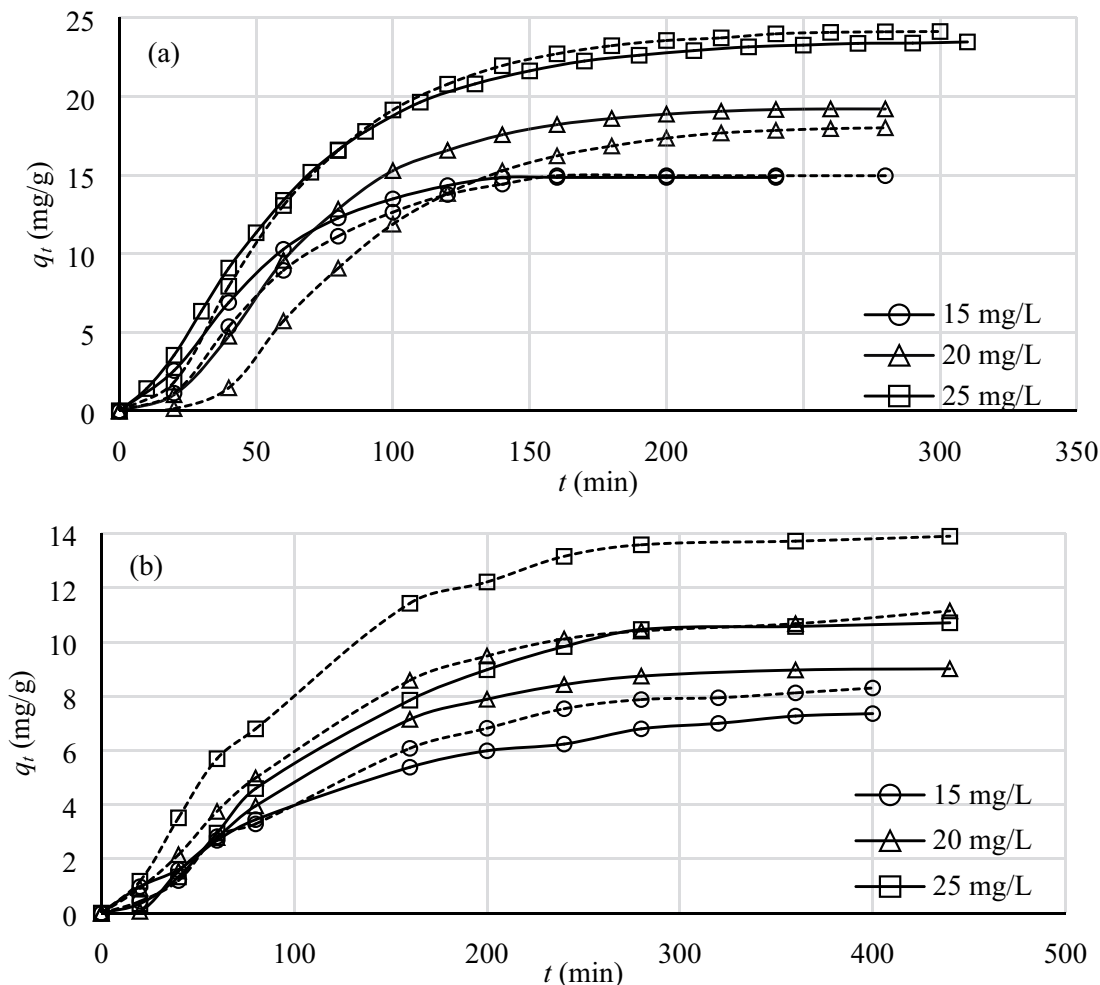
Fig. 4. Rate of dyes adsorption onto 3A-MS adsorbents (a) malachite green removal and (b) methyl violet removal (solid lines: 3A-MS, dashed lines: modified 3A-MS).

84% at C_0 = 100 mg/L before it suddenly drops to 44% at C_0 = 410 mg/L. A relatively poor performance was demonstrated by the adsorbents for methyl violet removal, whereby the highest achievable efficiency is only about 60% for the same concentration range.

Fig. 7 portrays the equilibrium curves of dyes adsorption by 3A-MS adsorbents. On molar basis, malachite green reveals a greater maximum capacity (0.50 mmol/g) with higher affinity towards 3A-MS adsorbents. Malachite green has two amine groups, namely tertiary aminic N and quinoniminic N, that could serve as the active centres for adsorption. However, the lone pair of quinoniminic N is delocalized over the ring, making it less susceptible to function. Likewise, methyl violet possesses three amine groups, two of which are quinoniminic N. As each dye carries only single active centre, the possible explanations for a higher malachite green adsorption over that of methyl violet are, (i) malachite green endows a smaller molecular diameter of 0.82 nm than methyl violet (1.24 nm), thus ensuring the molecules to diffuse much faster to reach the active sites, and (ii) the presence of extra quinoniminic group in methyl violet

might enfold some of the active sites, making them unreachable by free methyl violet molecules in bulk solution.

The equilibrium data were fitted into Langmuir model, and the calculated constants are summarized in Table 2. The Langmuir model has been widely used to describe the adsorption of water pollutants, and is given as, $q_e = Q_m b C_e / (1 + b C_e)$, where Q_m (mg/g) is the maximum adsorption capacity and b (L/mg) is the adsorption intensity. From Table 2, it was found that the equilibrium data obeyed the Langmuir model with regression > 0.93, even though the Q_m values are somewhat overestimated due to data scattering. Thus, the adsorption could be interpreted as the formation of monolayer accumulation of dye molecules on the homogeneous surface of 3A-MS adsorbents. Furthermore, malachite green reveals a greater magnitude of adsorption intensity, indicating a favourable adsorption at lower concentrations (≤0.2 mmol/L). As the adsorbents employed in this work are non-porous, the only possible dyes adsorption mechanisms could be synergistically governed by cation-exchange with sodium and potassium in the crystal matrix and electrostatic attraction with oxygen lone pair electrons [18,19].

Table 1
Pseudo-kinetics constants for dyes adsorption onto 3A-MS adsorbents

| C_0 (mg/L)	$q_{e,exp}$ (mg/g)	Pseudo-first-order			Pseudo-second-order		
		q_e (mg/g)	k_1 (1/min)	R^2	q_e (mg/g)	k_2 (g/mg min)	R^2
		Malachite green					
		3A-MS					
15	14.9	16.0	0.01633	0.9802	20.8	0.00072	0.9607
20	19.2	21.2	0.01074	0.9704	29.3	0.00030	0.9546
25	23.4	24.5	0.01306	0.9912	31.8	0.00038	0.9775
		Modified 3A-MS					
15	15.0	16.3	0.01313	0.9697	21.7	0.00053	0.9482
20	18.0	23.3	0.00640	0.9577	36.5	0.00012	0.9488
25	24.1	25.6	0.01216	0.9808	33.7	0.00032	0.9640
		Methyl violet					
		3A-MS					
15	7.36	7.90	0.00688	0.9983	11.0	0.00051	0.9962
20	8.97	10.2	0.00645	0.9817	14.5	0.00034	0.9697
25	10.6	12.4	0.00575	0.9825	18.1	0.00023	0.9724
		Modified 3A-MS					
15	8.31	9.54	0.00579	0.9897	14.0	0.00030	0.9838
20	11.2	12.0	0.00693	0.9916	16.7	0.00033	0.9825
25	13.9	14.8	0.00812	0.9927	19.0	0.00038	0.9820
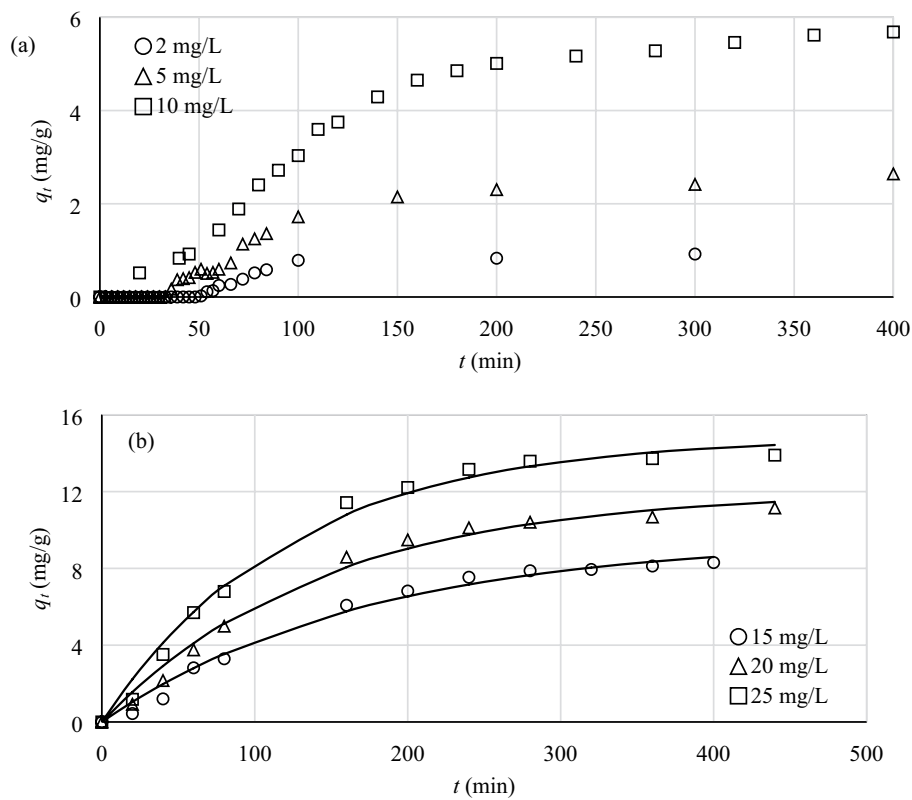
Fig. 5. Rate of (a) methyl violet and (b) malachite green adsorption at different concentrations by modified 3A-MS (lines were predicted by pseudo-first-order model).
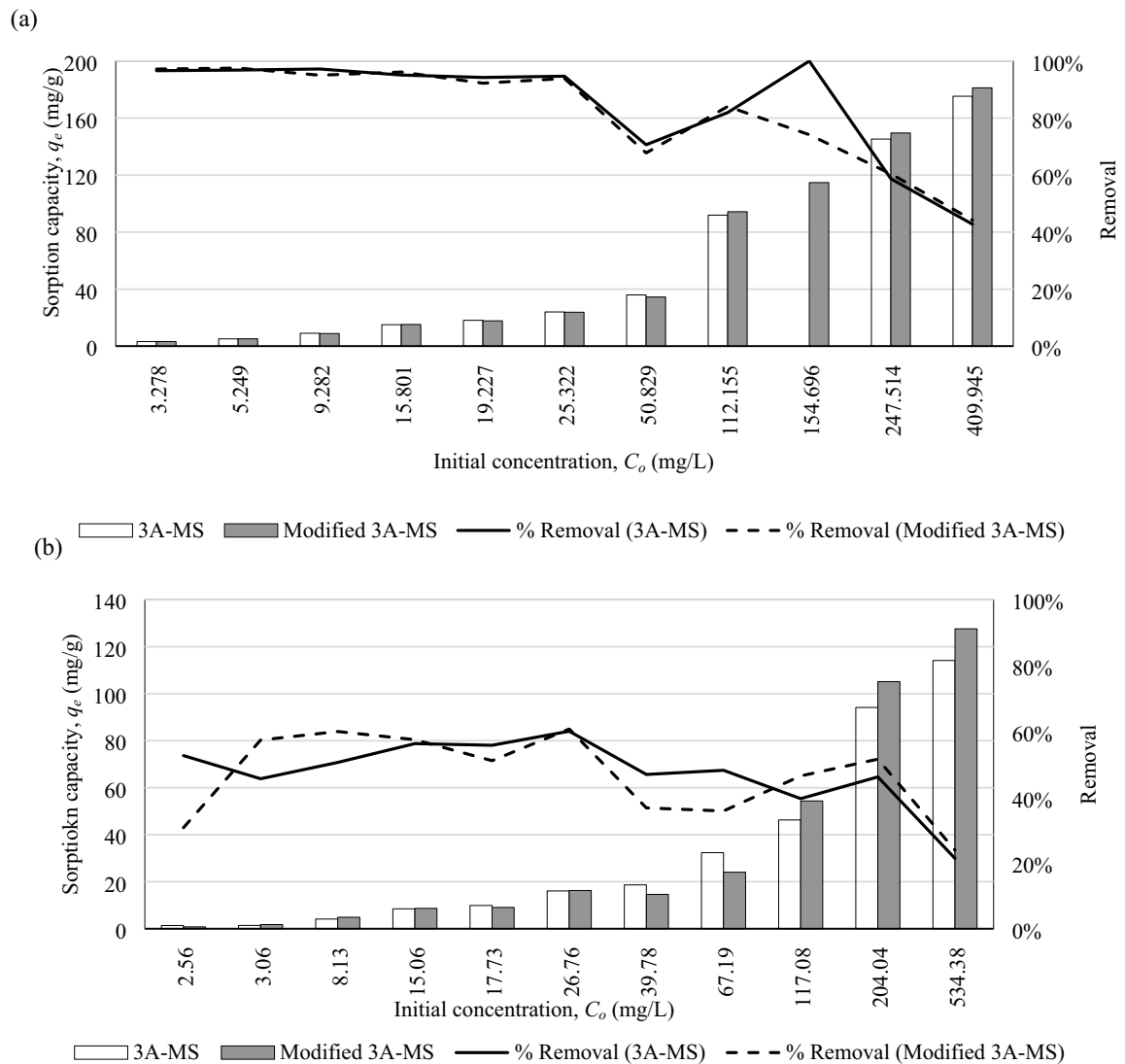
(a)

(b)

Fig. 6. Effect of dyes concentration on adsorption capacity and removal efficiency of 3A-MS adsorbents (a) malachite green adsorption and (b) methyl violet adsorption.

Table 2
Langmuir constants

	$Q_{m,\exp}$ (mg/g)	$Q_{m,\exp}$ (mmol/g)	Q_m (mg/g)	b (L/mg)	R^2
Malachite green					
3A-MS	181	0.495	199	0.029	0.967
Modified 3A-MS	186	0.510	206	0.029	0.958
Methyl violet					
3A-MS	126	0.320	149	0.009	0.963
Modified 3A-MS	136	0.345	177	0.008	0.928

Table 3 summarizes the removal of malachite green and methyl violet by various adsorbents. Malachite green and methyl violet are cationic dyes, and exhibit comparable characteristics. Generally, a high adsorption capacity of dye is well-connected to a high surface area of adsorbent with sufficient mesopore volume.

Waste apricot activated carbon (1,060 m²/g, 81% mesoporosity) recorded a malachite green adsorption capacity of 116 mg/g [23], while bentonite clay (46.6 m²/g) could only remove 7.72 mg/g at pH 9 [24]. The solution pH may also affect the removal of cationic dyes, as the basic environment favours the deprotonation of adsorbent surface, hence
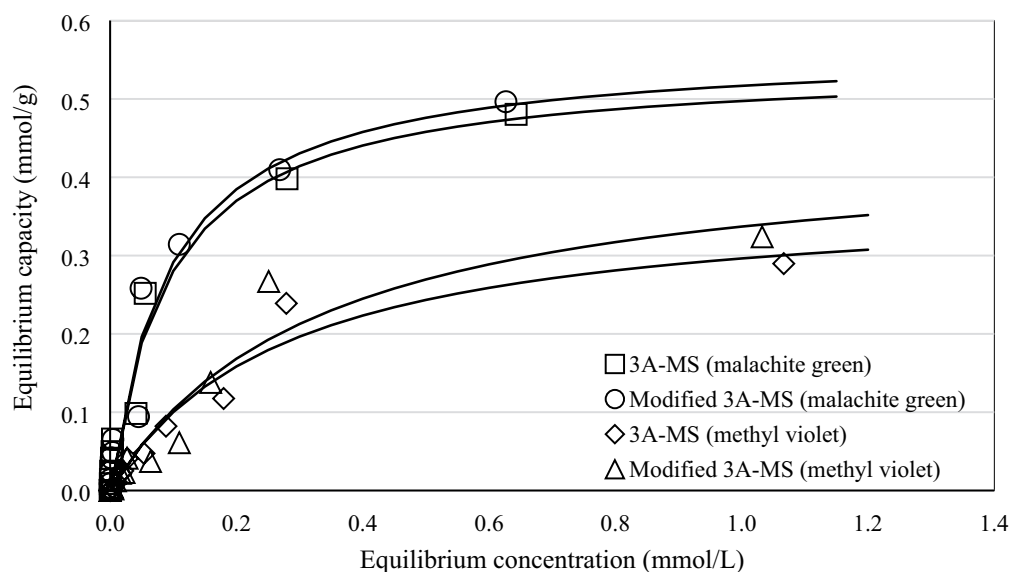
Fig. 7. Equilibrium adsorption of dyes onto 3A-MS adsorbents (lines were predicted by Langmuir model).

Table 3
Malachite green and methyl violet removal by various adsorbents

Adsorbent	Surface area (m²/g)	pH	Mesopore content (%)	Q_m (mg/g)	Reference
Malachite green					
Sphagnum peat moss-biomaterial	150	6.5	–	122	[20]
Activated carbon	1,000	7.0	25.4	149	[21]
Activated carbon derived from spent tea leaves	134	4.0	84.3	238	[22]
Waste apricot-based activated carbon	1,060	–	81	116	[23]
Bentonite clay	46.6	9.0	–	7.72	[24]
Degreased coffee beans	172	Natural	–	55.3	[25]
Treated ginger waste	–	9.0	–	84.0	[26]
Almond gum	–	7.0	–	172	[27]
Modified 3A-MS	0.1	Natural	–	186	This work
Methyl violet					
Granulated mesoporous carbon	900	7	–	203	[28]
Acid-modified activated carbon	676	7	8.56	83.3	[29]
Perlite	1.22	9	–	7.49	[30]
Bagasse fly ash	–	9	–	26.2	[31]
Sunflower seed hull	–	4.5	–	92.6	[32]
Almond shell	0.2	5.4	–	76.3	[33]
Modified 3A-MS	0.1	Natural	–	136	This work

creating a surface that is surrounded with OH– ions to instigate electrostatic attraction.

From Table 3, the 3A-MS adsorbents display better removal capacities for malachite green and methyl violet, even though the surface area is almost negligible. For malachite green adsorption, the maximum uptake of 3A-MS adsorbents outweighs that of activated carbons with superior surface area (Table 3). The inherent building matrix of 3A-MS allows the adsorption to take place via cationic-exchange and electrostatic interaction, without relying upon (meso)pore filling [34]. The present findings bring about the promising potential of 3A-MS adsorbent in dyes wastewater treatment.

4. Conclusion

3A-molecular sieve (3A-MS) and its NaOH-treated counterpart were used to challenge malachite green and methyl

violet in water. Generally, the modification shows some improvement on the removal capacities. On molar basis, 3A-MS adsorbents render a greater capacity with higher affinity for malachite green, which could be associated with the dye molecular properties. In this work, the maximum capacities were recorded as 126–136, and 181–186 mg/g for methyl violet and malachite green, respectively. As compared with the other adsorbents in literature, 3A-MS adsorbents exhibit a better performance, that could be governed by cation-exchange and electrostatic attraction. To conclude, 3A-MS adsorbents could be a promising adsorbent candidate for dyes wastewater treatment.

Acknowledgment

References

[1] S. Ming-Twang, Q. Zhi-Yong, L. Lin-Zhi, A.Y. Pei-Yee, M.A.A. Zaini, In: J.C. Taylor, Ed., Advances in Chemistry Research, Vol. 23, Nova Science Publishers Inc., New York, NY, 2015, pp. 143–156.

[2] T. Shu-Hui, M.A.A. Zaini, In: J.C. Taylor, Ed., Advances in Chemistry Research, Vol. 30, Nova Science Publishers Inc., New York, NY, 2016, pp. 19–34.

[3] M. Naushad, G. Sharma, Z.A. Alothman, Photodegradation of toxic dye using Gum Arabic-crosslinked-poly(acrylamide)/Ni(OH)$_2$/FeOOH nanocomposites hydrogel, J. Cleaner Prod., 241 (2019), doi: 10.1016/j.jclepro.2019.118263.

[4] S. Ming-Twang, L. Lin-Zhi, M.A.A. Zaini, Q. Zhi-Yong, A.Y. Pei-Yee, In: J.A. Daniels, Ed., Advances in Environmental Research, Vol. 36, Nova Science Publishers Inc., New York, NY, 2015, pp. 217–234.

[5] J. Mohanraj, D. Durgalakshmi, S. Balakumar, P. Aruna, S. Ganesan, S. Rajendran, M. Naushad, Low cost and quick time absorption of organic dye pollutants under ambient condition using partially exfoliated graphite, J. Water Process Eng., 34 (2019), doi: 10.1016/j.jwpe.2019.101078.

[6] T. Tatarchuk, N. Paliychuk, R.B. Bitra, A. Shyichuk, M. Naushad, I. Mironyuk, Adsorptive removal of toxic methylene blue and acid orange 7 dyes from aqueous medium using cobalt-zinc ferrite nanoadsorbents, Desal. Water Treat., 150 (2019) 374–385.

[7] G.B. Rao, M.K. Prasad, C.-H.V.R. Murthy, Cobalt(II) removal from aqueous solutions by adsorption onto molecular sieves, Int. J. Chem. Sci., 13 (2015) 1893–1910.

[8] N. Sun, P. Bai, X. Guo, L. Wang, Removal of water from anisole by 3A molecular sieve in batch and fixed-bed column systems, Asian J. Chem., 26 (2014) 2839–2844.

[9] J.B. Lad, Y.T. Makkawi, Adsorption of dimethyl ether (DME) on zeolite molecular sieves, Chem. Eng. J., 256 (2014) 335–346.

[10] A.T. Shah, M.I. Din, F.N. Kanwal, M.L. Mirza, Direct synthesis of mesoporous molecular sieves of Ni-SBA-16 by internal pH adjustment method and its performance for adsorption of toxic brilliant green dye, Arabian J. Chem., 8 (2015) 579–586.

[11] Z.H. Li, Z.C. Wang, G. Li, Y.C. Liu, Synthesis of mesoporous molecular sieve MCM-41 and its adsorption behavior for rhodamine B, Adv. Mater. Res., 893 (2014) 658–663.

[12] A. Ates, Effect of alkali-treatment on the characteristics of natural zeolites with different compositions, J. Colloid Interface Sci., 523 (2018) 266–281.

[13] M. Ogura, S.-Y. Shinomiya, J. Tateno, Y. Nara, M. Nomura, E. Kikuchi, M. Matsukata, Alkali-treatment technique – new method for modification of structural and acid-catalytic properties of ZSM-5 zeolites, Appl. Catal., A, 219 (2001) 33–43.

[14] C. Zou, P. Zhao, M. Wang, D. Liu, H. Wang, Z. Wen, Failure analysis and faults diagnosis of molecular sieve in natural gas dehydration, Eng. Fail. Anal., 34 (2013) 115–120.

[15] M. Rahmani, M. Kaykhaii, M. Sasani, Application of Taguchi L16 design method for comparative study of ability of 3A zeolite in removal of rhodamine B and malachite green from environmental water samples, Spectrochim. Acta A, 188 (2018) 164–169.

[16] B.R. Gaddala, K.P. Monditoka, V.R.M. Challa, K.K. Kadimpati, Potential use of molecular sieves for the removal of Ni^{2+} metal ion: kinetics, isotherms and thermodynamic studies, J. Inst. Eng. (India), Ser. E, 97 (2016) 183–192.

[17] M.A. Hubbe, S. Azizian, S. Douven, Implications of apparent pseudo-second-order adsorption kinetics onto cellulosic materials: a review, BioResources, 14 (2019) 7582–7626.

[18] N.B. Swan, M.A.A. Zaini, Adsorption of malachite green and congo red dyes from water: recent progress and future outlook, Ecol. Chem. Eng., S26 (2019) 119–132.

[19] J.A. Alexander, M.A.A. Zaini, A. Surajudeen, E.-N.U. Aliyu, A.U. Omeiza, Surface modification of low-cost bentonite adsorbents – a review, Part. Sci. Technol., 37 (2019) 534–545.

[20] F. Hemmati, Z. Norouzbeigi, F. Sarbisheh, H. Shayesteh, Malachite green removal using modified sphagnum peat moss as a low-cost biosorbent: kinetic, equilibrium and thermodynamic studies, J. Taiwan Inst. Chem. Eng., 58 (2016) 482–489.

[21] Y. Onal, C. Akmil-Başar, C. Sarici-Ozdemir, Investigation kinetics mechanisms of adsorption malachite green onto activated carbon, J. Hazard. Mater., 146 (2007) 194–203.

[22] E. Akar, A. Altinisik, Y. Seki, Using of activated carbon produced from spent tea leaves for the removal of malachite green from aqueous solution, Ecol. Eng., 52 (2013) 19–27.

[23] C.A. Basar, Applicability of the various adsorption models of three dyes adsorption onto activated carbon prepared waste apricot, J. Hazard. Mater., 135 (2006) 232–241.

[24] S.S. Tahir, N. Rauf, Removal of a cationic dye from aqueous solutions by adsorption onto bentonite clay, Chemosphere, 63 (2006) 1842–1848.

[25] M.-H. Baek, C.O. Ijagbemi, S.-J. O, D.S. Kim, Removal of malachite green from aqueous solution using degreased coffee bean, J. Hazard. Mater., 176 (2010) 820–828.

[26] R. Ahmad, R. Kumar, Adsorption studies of hazardous malachite green onto treated ginger waste, J. Environ. Manage., 91 (2010) 1032–1038.

[27] F. Bouaziz, M. Koubaa, F. Kallel, R.E. Ghorbel, S.E. Chaabouni, Adsorptive removal of malachite green from aqueous solutions by almond gum: kinetic study and equilibrium isotherms, Int. J. Biol. Macromol., 105 (2017) 56–65.

[28] Y. Kim, J. Bae, H. Park, J.-K. Suh, Y.-W. You, H. Choi, Adsorption dynamics of methyl violet onto granulated mesoporous carbon: facile synthesis and adsorption kinetics, Water Res., 101 (2016) 187–194.

[29] A.T.M. Din, B. Hameed, Adsorption of methyl violet dye on acid modified activated carbon: isotherms and thermodynamics, J. Appl. Sci. Environ. Sanitation, (2010) 151–160, doi: 10.13140/2.1.4382.2882.

[30] M. Dogan, M. Alkan, Adsorption kinetics of methyl violet onto perlite, Chemosphere, 50 (2003) 517–528.

[31] I.D. Mall, V.C. Srivastava, N.K. Agarwal, Removal of orange G and methyl violet dyes by adsorption onto bagasse fly ash - kinetic study and equilibrium isotherm analyses, Dyes Pigm., 69 (2006) 210–223.

[32] B.H. Hameed, Equilibrium and kinetic studies of methyl violet sorption by agricultural waste, J. Hazard. Mater., 154 (2008) 204–212.

[33] C. Duran, D. Ozdes, A. Gundogdu, H.B. Senturk, Kinetics and isotherm analysis of basic dyes adsorption onto almond shell (Prunus dulcis) as a low cost adsorbent, J. Chem. Eng. Data, 56 (2011) 2136–2147.

[34] M. Naushad, A. Mittal, M. Rathore, V. Gupta, Ion-exchange kinetic studies for Cd(II), Co(II), Cu(II), and Pb(II) metal ions over a composite cation exchanger, Desal. Water Treat., 54 (2015) 2883–2890.